HHS Public Access

Author manuscript

J Cogn Neurosci. Author manuscript; available in PMC 2018 June 28.

Published in final edited form as:

J Cogn Neurosci. 2018 February ; 30(2): 256–266. doi:10.1162/jocn_a_01198.

Spatially Selective Alpha Oscillations Reveal Moment-by-Moment Trade-offs between Working Memory and Attention

Dirk van Moorselaar[1], **Joshua J. Foster**[2], **David W. Sutterer**[2], **Jan Theeuwes**[1], **Christian N. L. Olivers**[1], and **Edward Awh**[2]

[1]Vrije Universiteit Amsterdam

[2]The University of Chicago

Abstract

Current theories assume a functional role for covert attention in the maintenance of spatial information in working memory. Consistent with this view, both the locus of attention and positions stored in working memory can be decoded based on the topography of oscillatory alpha-band (8–12 Hz) activity on the scalp. Thus far, however, alpha modulation has been studied in isolation for covert attention and working memory tasks. Here, we applied an inverted spatial encoding model in combination with EEG to study the temporal dynamics of spatially specific alpha activity during a task that required observers to visually select a target location while maintaining another independently varying location in working memory. During the memory delay period, alpha-based spatial tuning functions shifted from the position stored in working memory to the covertly attended position and back again after the attention task was completed. The findings provide further evidence for a common oscillatory mechanism in both the selection and the maintenance of relevant spatial visual information and demonstrate the dynamic trade-off in prioritization between two spatial tasks.

INTRODUCTION

Spatial working memory (WM), the ability to hold relevant spatial information online, and spatial attention, the ability to focus cognitive resources on relevant locations while ignoring other locations, are thought to share underlying mechanisms. At a neurophysiological level, both processes are driven by a right-hemisphere dominant network of frontal and parietal nodes (Awh & Jonides, 1998; Awh, Smith, & Jonides, 1995). At a functional level, covertly shifting attention away from a memorized location impairs spatial memory performance (Awh, Jonides, & Reuter-Lorenz, 1998). These and other findings have led to the idea that WM is an emergent property of attentional mechanisms that sustain activity in sensory regions (Kiyonaga & Egner, 2013; Olivers, 2008; Postle, 2006; Theeuwes, Olivers, & Chizk, 2005; Awh & Jonides, 2001). In this view, covert attention toward a location plays a functional role in the maintenance of information in spatial WM.

Reprint requests should be sent to Dirk van Moorselaar, Department of Cognitive Psychology, VU University, Van der Boechorststraat 1, 1081 BT Amsterdam, the Netherlands, or via dirkvanmoorselaar@gmail.com.

The idea that spatial attention and spatial WM are intrinsically related is further supported by the observation that both are associated with spatially specific modulations of posterior alpha oscillations (8–12 Hz) in EEG/MEG signals. Specifically, the topographic distribution of alpha power tracks both the attended visual hemifield (Gould, Rushworth, & Nobre, 2011; Kelly, Lalor, Reilly, & Foxe, 2006) as well as the hemifield of a remembered stimulus (van Dijk, van der Werf, Mazaheri, Medendorp, & Jensen, 2010; Medendorp et al., 2007) via contralateral alpha suppression in posterior electrodes. This location specificity of alpha-band dynamics is not limited to the hemifield level but also tracks the specific location that is attended (Foster, Sutterer, Serences, Vogel, & Awh, 2017; Rihs, Michel, & Thut, 2007). Indeed, recent studies have used inverted encoding models (IEMs) to reconstruct population-level channel tuning functions (CTFs) from the topographic distribution of alpha-band activity that reveal location-specific information during both covert attention tasks (Foster et al., 2017; Samaha, Sprague, & Postle, 2016) and the maintenance of spatial working memories (Foster, Bsales, Jaffe, & Awh, 2017; Foster, Sutterer, Serences, Vogel, & Awh, 2016). Together, these findings suggest a tight link between alpha-band dynamics and the focus of spatial attention, regardless of whether attention is directed toward external stimuli or toward remembered locations.

However, although alpha-band topography has proven to be useful in tracking the allocation of both attentional and WM resources, so far the alpha modulations associated with these tasks have been studied in isolation. It thus remains unclear whether the maintenance of information in WM is in direct competition with the covert selection of positions in the external environment. Behavioral evidence suggests that this is not necessarily the case. For example, a number of studies have shown that WM maintenance is unaffected (or only modestly affected) by an intervening visual search task, and, likewise, a concurrent WM load does not reduce visual search efficiency (Hollingworth & Maxcey-Richard, 2013; Woodman, Vogel, & Luck, 2001). However, the lack of such a behavioral effect in itself does not rule out strong functional overlap between WM maintenance and visual attention. Another possibility is that spatial attention is integral to storage in spatial WM, but that when a WM task is interrupted by a task that also requires attention, observers are able to temporarily drop the information from WM and then reactivate the needed information when the resources for online storage are available again. Thus, to distinguish between these possibilities, we examined whether the neural signals tracking online memory representations were maintained when observers were required to direct attention externally to an independent location. If the maintenance of information within WM is in direct competition with covert selection, we would expect a trade-off between WM and covert attention such that the WM representation will be impaired during the attention task. Alternatively, if WM maintenance is independent from covert selection, we should be able to simultaneously reconstruct the memorized location and the attended location without any costs.

To this end, we measured EEG while participants performed a dual spatial WM and covert attention task. In the crucial condition, the participants performed a cued target detection task during the delay period of the spatial memory task (see Figure 1 for an illustration of the procedure). A control condition used identical displays, but here, observers ignored the intermediate attention task and focused only on the memory task. We used a spatial IEM to

reconstruct the neural representation of the memorized and the cued location across conditions based on the topography of alpha activity on the scalp (Foster et al., 2016). Specifically, we modeled the relationship between neural activity and spatial locations via a hypothesized response profile (Brouwer & Heeger, 2009, 2011), which was then used to reconstruct location-selective CTFs. These CTFs allowed us to track the time course of active maintenance in spatial WM when participants were required to direct covert attention toward an independent location during the delay period. Thus, by examining spatially selective alpha-band activity, we were able to test whether covert orienting to the intervening task interrupted the active representation in spatial WM, as would be the case if covert orienting and spatial WM rely on the same mechanism. Alternatively, the intervening attention task might leave the CTFs for the memorized location undisturbed, implying independent resources for WM and attention (Hollingworth & Maxcey-Richard, 2013; Woodman et al., 2001).

METHODS

Participants

A planned number of 16 healthy volunteers (ages 18–34 years, four men), all right-handed, participated, in exchange for course credit or monetary compensation. Five participants were replaced because too many trials (>30%) were lost due to recording or ocular artifacts. Participants reported normal or corrected-to-normal vision and provided informed consent according to procedures approved by the Scientific and Ethical Review Committee (Faculty of Behavioral and Movement Sciences, VU University).

Stimulus Displays

Stimuli were created using OpenSesame version 3.0.2 (Mathôt, Schreij, & Theeuwes, 2012), a Python-based graphical experiment builder, and were presented on a 22-in. video monitor (Syncmaster 2233, Samsung, Seoul, South Korea; resolution: 1680 × 1050 pixels, refresh rate: 120 Hz) at ~100 cm viewing distance. All stimuli, except for the spatial cues, were rendered in dark gray against a medium gray background.

The spatial WM task was modeled after Foster et al. (2016) and required participants to remember the angular location of a circle stimulus. The circle (1.4° in diameter) was centered 3.6° of visual angle from the central fixation point (0.1° in diameter). The angular location was randomly sampled from one of eight location bins spanning 0–315°, in steps of 45°, with jitter added to cover all 360° of possible locations to prevent categorical coding of the location. At test, participants used a mouse to click on the perimeter of a probe ring (7.2° in diameter).

The intermediate attention task required participants to detect a randomly selected target digit (2, 3 or 5) in one of eight colored boxes (1.0° × 1.0°). The boxes were centered at 2.0° eccentricity, at fixed locations spanning 22.5–337.5°, in steps of 45°. On each trial, the outlines of these boxes were colored by random selection from a color pool with eight different colors (red, green, blue, cyan, yellow, purple, orange, pink). One of these colors signaled the target location with 87.5% probability. The location of target and the to-be-

memorized location varied independently. Boxes without a digit contained a randomly selected letter (E, H, P), with a maximum of three identical letters per display. Target stimuli were only visible for a limited period before filling up all line segments that made up the digits and letters, creating a box-figure eight, which remained on screen until test display onset.

Task Design

Each trial started with a 250-msec blank display, followed by fixation dot for a randomly jittered duration of 600–1500 msec. Next, a memory display was presented for 200 msec (Figure 1). The memory item consisted of a single disk presented at a single location. In addition to the disk, but irrelevant to the memory task, this display also contained eight colored boxes. Participants were instructed to ignore the boxes and remember the angular location of the disk. These boxes remained visible throughout the trial, until the memory test. One second after the offset of the sample stimulus, these boxes were filled with letters and were subsequently masked. In the dual-task condition, participants had to covertly attend to one of the colored boxes to detect a target digit. In the dual-task condition, one of the characters in the search display was a digit, which on each trial could be a 2, 3, or 5 (these numbers were selected as they consisted of equal number of line segments). In valid trials (87.5%), a target digit appeared in the cued box (e.g., green, which remained fixed throughout the experiment; counterbalanced across participants). In invalid trials, the target was presented in one of the randomly selected non-cued boxes. This allowed us to establish whether participants indeed attended the cued location during the intermediate task. In the dual-task condition, participants had 1000 msec to indicate the target digit by button press, whereas in the single-task condition, participants were instructed to ignore the displays associated with the intermediate task. Each trial ended with the presentation of the memory test, which was visible until response. The test display did not contain a fixation circle, and participants were free to move and blink their eyes once it had appeared. Participants were instructed to report the location of the remembered stimulus as precisely as possible.

Procedure

After providing informed consent, participants were fitted with a 64-electrode cap and six face electrodes. Testing took place in a dark, electrically shielded chamber. Before starting the experiment, participants completed a set of five practice trials for each task (i.e., memory task and covert attention task) separately. They then completed a series of 15 practice trials until they felt comfortable with the dual-task structure. Once participants were ready to start the experiment, they first completed a separate block of 64 trials, including the covert attention task to determine the SOA between target and mask display. For this purpose, we used a weighted up–down staircase (Kaernbach, 1991; start = 104, step = 8, min value = 24, max value = 175), which was only updated on valid cue trials. Subsequently, participants completed 26 blocks of 64 trials each. Each participant completed 13 dual-task and 13 single-task blocks, in counterbalanced order. After each block, feedback was given on memory performance; in dual-task blocks, feedback was also given on intermediate task performance. Participants were encouraged to take a break in between blocks. The experiment took approximately 3–3.5 hr to complete.

Modeling the Response Error Distribution

Response error on each trial was calculated by taking the angular difference between the reported and presented location. For each participant, the resulting error distribution, ranging from −180° to 180°, was modeled as the mixture of a von Mises distribution and a uniform distribution (Zhang & Luck, 2008). Using the MemToolbox (Suchow, Brady, Fougnie, & Alvarez, 2013), we obtained maximum likelihood parameters for three parameters: (1) the mean of the von Mises distribution, corresponding to response bias; (2) the dispersion of the von Mises distribution (sd), corresponding to mnemonic precision; and (3) the height of the uniform distribution (P_f), corresponding to the probability of forgetting the sample stimulus.

EEG Acquisition and Preprocessing

We recorded EEG at 512 Hz using a 64-electrode cap with the electrodes placed according to the extended 10–20 system (using a BioSemi ActiveTwo system; Amsterdam, The Netherlands; biosemi.com). All sites were re-referenced to the average of left and right mastoids. In addition, vertical EOG was recorded from electrodes located 2 cm above and below the right eye, and horizontal EOG (HEOG) was recorded from electrodes 1 cm lateral to the external canthi. Continuous EEG was epoched from −800 to 2700 msec, relative to memory display onset. The resulting epochs were baseline-normalized using the whole epoch as baseline. Before cleaning, the data were visually inspected for malfunctioning electrodes with excessive noise, which were removed from the data (M = 9, min = 5, max = 17). Each epoch (−300:2200 msec) was carefully screened for blocking eye-related and muscle-related artifacts with visual inspection using EEGLAB via Matlab 2014b (The MathWorks, Natick, MA), leaving an average of 1362 artifact-free trials perparticipant andanaverageof694 (min=625,max=987) and 668 (min = 493, max = 792) observations for single- and dual-task conditions, respectively. Removal of ocular artifacts was effective: Variation in the grand-averaged HEOG waveforms by cued location or memorized location was smaller than 2 μV, indicating that the residual variation in the average HEOG corresponds to variations in eye position smaller than 0.2° of visual angle (see Lins, Picton, Berg, & Scherg, 1993, for a demonstration that eye movements of about 1° of visual angle produce a deflection in the HEOG of approximately 16 μV). All other analyses were performed using MNE software (Gramfort et al., 2013) and custom code running in a Python environment (Python Software Foundation, https://www.python.org/).

Multivariate Inverted Encoding Mode (IEM)

Following Foster et al. (2016), we used an inverted spatial encoding model to reconstruct location-selective CTFs via topographic power distributions of the EEG signal. Analyses presented here are based on posterior electrodes only[1] (i.e., 32 posterior electrodes; M = 26, min = 21, max = 29). The IEM procedure was run separately for the memory and the cue location.[2]

[1]Analyses including all electrodes resulted in virtually identical results, indicating that most, if not all, information was represented in posterior electrodes.

[2]All data and materials have been made publicly available via the Open Science Framework and can be accessed at https://osf.io/56rzh.

To isolate frequency-specific activity, the preprocessed EEG signal was filtered using a fifth-order butterworth bandpass filter within MNE. For the time–frequency analysis, we searched a broad range of frequencies (4–34 Hz, in increments of 2 Hz with a 4-Hz band; 4–8 Hz, 6–10 Hz, etc.). Subsequently, evoked power and total power were calculated after extraction of the complex analytic signal via a Hilbert transform. Evoked power was computed by averaging the complex analytical signal across trials before squaring the complex magnitude of the analytic signal, whereas this averaging was done after power subtraction for total power. Consequently, evoked power reflects activity phase-locked to stimulus onset, and total power reflects ongoing activity irrespective of its phase relationship to the onset of the memory stimulus.

Before calculating evoked power, artifact-free trials were partitioned without replacement into three blocks. To prevent bias in the analysis, we equated the number of observations across locations (i.e., memory and cue locations) and conditions. As a result, a random subset of trials was not included in any block. To account for this, we randomly generated multiple block assignments. For time–frequency analysis and alpha-band analysis (8–12 Hz), we used respectively 5 and 10 block assignments. For each new block assignment, evoked power and total power were calculated for each location bin for each block, resulting in an $l \times b \times m \times s$ matrix of both evoked power and total power for both conditions, where l is the number of location bins, b is the number of blocks, m is the number of electrodes, and s is the number of time samples. This matrix served as input to the IEM routine.

Following similar approaches (Brouwer & Heeger, 2009, 2011), we modeled the response profile of each spatial channel across angular locations as a half sinusoid raised to the seventh power and centered on each polar angle (i.e., 0°, 45°, 90°, etc.). An IEM routine was then applied to each time–frequency point in the time–frequency analysis and to each time point in the alpha-band analysis in two stages. In the first stage, training data from two out of the three blocks were used in a general linear model of the form:

$$B_1 = WC_1$$

where B_1 (m electrodes × n trials) is the observed power (evoked or total) at each electrode for each trial in the training set, C_1 (k channels × n trials) is a matrix of predicted responses for each information channel on each trial, and W is a weight matrix that characterizes the mapping from “channel space” to “electrode” space. The weight matrix W was obtained via least-squares estimation with python function np.linalglstsq(C_1, B_1). Next, in the test phase, the model was inverted to transform the observed test data B_2 (m electrodes × n_2 trials) into a set of estimated channel responses C_2 (k channels × n_2 trials), via the python function np.linalg.lstsq(W.T, B_2.T). Each estimated channel response was circularly shifted to a common center (0°) and averaged across trials.

This procedure was iterated in a “leave-one-out” cross-validation routine where two blocks of estimated power values served as B_1 and the remaining block served as B_2 until each block served as a test set (i.e., as B_2). Thus, the training and the test data were always independent. To construct tuning functions over time (Figures 3–6), this procedure was

performed for every sample, and the resulting CTFs were averaged across each test block in all block assignments.

Alpha-band Cross-training

To examine whether storage in WM and covert attention rely on common oscillatory mechanisms, we examined cross-task generalization. We repeated the IEM model on total power, with 10 block assignments, but now only using memory locations as training data and cue locations as test data. For this purpose, the centers of the eight memory bins were shifted 22.5° to align them to the locations of the colored boxes. The IEM procedure was then repeated for every combination of time points resulting in a generalization across time points matrix with CTF slopes. This analysis was performed twice, once using memory locations from the single-task blocks and once using memory locations from the dual-task blocks.

Statistical Analysis

In the first step of the analysis, we used a one-sample *t* test to test which frequency bands showed spatial selective CTFs across conditions. For this purpose, we used linear regression to estimate CTF slopes (i.e., slope of channel response as a function of location channels after collapsing across channels that were equidistant from the center of the response function) and tested whether these slope estimates were reliably larger than zero with a Monte Carlo randomization procedure. Specifically, we repeated the IEM, as described in the IEM and the alpha-band cross-training paragraphs, 500 times, but with randomized location labels to obtain a null distribution of *t* statistics. Then, we calculated the probability of obtaining a *t* statistic from the surrogate null distribution greater than or equal to the observed *t* statistic (i.e., the probability of a Type 1 error). CTF selectivity was deemed reliably above chance if the probability of a Type 1 error was less than .01. This procedure was used in the time–frequency analysis and the alpha-band cross-training analysis.

Next, we used group-level permutation testing with cluster correction to test whether there were reliable condition differences. This nonparametric method corrects for multiple comparisons by taking into account autocorrelation in time and frequency (Cohen, 2014; Maris & Oostenveld, 2007). The sign of the slope difference between conditions was randomly shuffled in 1000 iterations, and these randomizations were used to compute significant clusters of time–frequency points (or time points for the alpha band analysis; $p < .05$). At the same time, for each permutation, the size of the largest time–frequency cluster was determined, resulting in a distribution of maximal cluster sizes under the null hypothesis of no-condition differences. The sizes of the significant clusters of the non-permuted data were thresholded such that only clusters larger than the 95th percentile of the surrogate distribution were considered reliable ($p < .05$).

RESULTS

Behavior

Figure 2 shows the mnemonic precision and probability of forgetting the stimulus as computed with a mixture model across conditions. Although the numerical difference

between conditions was very small, planned pairwise comparisons demonstrated that these differences were reliable. When participants performed the dual-task condition, both mnemonic precision, $F(1, 15) = 22.671$, $p < .001$, and the probability of recalling the memorandum, $F(1, 15) = 15.180$, $p = .001$, decreased relative to the single-task condition. Note that, at just over 1%, the probability that participants could not recall the item was still extremely low even in the dual-task condition. Response bias did not differ across conditions ($F = 0.170$, $p = .69$).

The covert attention task showed a clear cue validity effect in target identification: Participants responded faster and more accurately on valid (mean RT ± *SD*: 615 ± 55 msec; mean proportion correct ± *SD*: 0.84 ± 0.08) than on invalid trials (mean RT = 666 ± 58 msec; mean proportion correct = 0.41 ± 0.06), $F(1, 15) = 60.792$, $p < .001$, and $F(1, 15) = 632.295$, $p < .001$, respectively. Thus, participants did indeed attend the cued location.

EEG-based CTFs

We performed a permutation test at each time–frequency point to identify time points at which the spatial selectivity (measured as CTF slope, see Methods) of the reconstructed CTF profile was reliably above zero (i.e., points where the CTF profile was not flat). First, we analyzed which frequency bands were sensitive to the memorized location in terms of their topographic distribution. Figure 3A shows the temporal evolution of the reconstructed CTFs in the single-task condition. Replicating Foster et al. (2016), a range of low frequencies (4–15 Hz) transiently tracked, both via evoked power and total power, the memory location during stimulus presentation. Only total alpha power (8–12 Hz) enabled reliable CTF reconstruction throughout the entire delay period. A different pattern was observed in the dual-task condition (Figure 3B), where total alpha power CTF reconstruction was disrupted around the target display onset of the intermediate attention task and only became reliable again about 600 msec later. A cluster-based permutation test confirmed that, immediately after target display onset of the intermediate attention task, total alpha power CTF slopes were reliably larger in the single-task than in the dual-task condition ($p < .05$). Interestingly, the same analysis indicated that CTF slopes started to differ between the single- and dual-task conditions *before* the target display onset (white outline Figure 3B), suggesting that about 500 msec after memory encoding observers switched attention to the cued location in anticipation of the target display.

The results revealed an interruption of the spatially selective alpha activity that tracked the memory position when participants were required to perform an intermediate task that required covert attention. Next, we examined whether spatially selective alpha activity also tracked the position that participants were cued to attend during the intervening task. As Figure 4 shows, we observed a robust CTF that tracked the covertly attended position, but only in the dual-task condition when that position was relevant. In the single-task condition (in which the cued location was irrelevant), there was no evidence for a reliable reconstruction of the cued location, except for a small hint in low frequency evoked power (4–6 Hz) immediately after stimulus onset (Figure 4A, top left). By contrast, in the dual-task condition, both evoked power and total power showed clear location-specific CTFs for the target location of the intervening attention task (Figure 4B). Total alpha power contained

location-specific information already before target display onset, which remained reliable until after the response. Cluster-based permutation tests confirmed that CTF slopes were reliably steeper in the dual-task than in the single-task condition, both for evoked power and total power (Figure 4B, white outline). Importantly, for total power, this difference started to be reliable around the same time frame when CTF slopes tuned to the memorized location started to differentiate. In other words, the alpha-based CTFs for the intermediate attention task emerged when the CTFs for the memory task waned. This is also clear in Figure 5, which visualizes the CTF slopes as obtained by the alpha-band analysis. The time course of spatially selective alpha activity suggests a moment-by-moment trade-off between storage in WM and covert attention toward a separate location.

The moment-by-moment trade-off between storage in WM and covert attention is in line with the idea that both rely on a common oscillatory process. To provide converging evidence for this idea, we examined whether we could cross train between the two types of tasks. The logic here is that if WM storage and covert attention indeed recruit common oscillatory mechanisms, it should be possible to reconstruct the cued location in the covert attention task based on a model that is trained on memorized locations (see Methods section for details). Indeed, as visualized in Figure 6, memory locations could be used to reconstruct the cued location for the time window where total alpha power carried information about the cued location in the dual task (notably between about 800 and 1500 msec). Importantly, and consistent with the waxing and waning of alpha CTFs in the dual-task memory locations of the single task resulted in reliable CTF slopes, regardless of which exact time point in the maintenance interval was used during training (Figure 6A), whereas dual-task memory locations only resulted in reliable reconstructions at the start and end of the maintenance interval, resulting in a gap in decoding accuracy when observers are turning to the covert attention task (Figure 6B). Note further that a more sustained across-task reconstruction emerged around the average RT. As shown in Figure 5, this is also the time when CTF reconstruction for the attention task was strongest, suggesting that observers were most focussed on the target location at the time of response. The strong signal around response meant that attention-based CTFs could be reconstructed based on a memory-based model, even though the memory-based CTFs were considerable weakened for this same time period.

Another interesting aspect of the data is that evoked power in the lower end of the frequency spectrum (~4–8 Hz) also tracked the position of the cued position and the subsequent target starting at onset and peaking about 200 msec after the offset of the cue or target. In a recent study, Dowdall, Luczak, and Tata (2012) suggested that evoked posterior theta activity underlies the N2pc, a lateralized ERP component occurring 200–300 msec after stimulus onset that is thought to reflect the orienting of attention (Luck & Hillyard, 1990). Consistent with such a mechanism, we found that location-specific theta activity peaked around the same time frame as the typical N2pc (i.e., about 250 msec after display onset). Interestingly, in the dual-task condition, evoked theta activity supported reliable reconstruction of both the to-be-memorized and cued locations immediately following memory display onset (Figures 3B and 4B, top right). The cue-based activation was not stimulus-driven, as the cue was presented within a circular configuration of colored boxes. This suggests that, even though participants could in principle ignore the cued box during memory encoding, it nevertheless

captured attention on the basis of its prospective task relevance. Although this was especially clear in the dual-task condition, even in the single-task condition there was a small hint of statistically reliable activity tracking the cue location after memory display onset even though the cue was irrelevant in this condition. Possibly in a small subset of trials, the cue automatically captured attention on the basis of its task relevance in the preceding dual-task blocks.

DISCUSSION

Previous work has demonstrated that the topography of alpha-band power tracks the locus of spatial attention with relatively fine temporal resolution during both orienting toward external positions (Foster et al., 2017; Samaha et al., 2016; Rihs et al., 2007) and the maintenance of positions in WM (Foster et al., 2016). These studies made use of spatial IEMs tailored to reconstruct CTF profiles from activity in location-tuned neural populations. Here, we used the same method to test whether covert shifts of attention during a WM delay period disrupt the representation of the memorized location. We found that population-level neural activity in the alpha band supported robust spatial tuning for both covertly attended and memorized locations, but the spatial tuning profiles showed a clear trade-off between the memory and covert orienting goals of the task. When observers had to perform a covert attention task, memory-related signals dissipated until after the intervening attention task had been completed. This finding indicates that spatial WM and spatial attention recruit a common alpha-band mechanism.

Although covert orienting during the delay period disrupted the spatial representation of the remembered location, this representation reemerged after the attention task was completed. This suggests that observers must have temporarily maintained the memorandum via a mechanism other than active maintenance—one that potentially functions in the absence of sustained focused attention (Hollingworth & Maxcey-Richard, 2013). This empirical pattern is reminiscent of earlier work in which decoding accuracy for items stored in WM declined to baseline levels when participants were instructed that those items would only be potentially relevant later, after another task had been completed first (LaRocque, Riggall, Emrich, & Postle, 2016; LaRocque, Lewis-Peacock, Drysdale, Oberauer, & Postle, 2013; Lewis-Peacock, Drysdale, Oberauer, & Postle, 2012). The same items could be successfully decoded again once the first task was completed and attention was redirected to the remembered items. Furthermore, recent work has shown that alpha activity provides a sensitive index of the relative prioritization of currently relevant memories over memories that only become relevant later, when the first task is completed (de Vries, van Driel, & Olivers, 2017).

These findings and the fact that covert orienting (in the dual-task condition) produced only a modest cost in location report performance raise the question as to what the functional role of the information carried in alpha oscillations is. In other words, which mnemonic mechanism enables storage when the memorandum is not within the current focus of attention? As an alternative to sustained activity-driven WM mechanism, some have hypothesized “activity silent” representations that are maintained via temporary changes in synaptic weights between the relevant neural units (Rose et al., 2016; Stokes, 2015; Olivers,

Peters, Houtkamp, & Roelfsema, 2011; Mongillo, Barak, & Tsodyks, 2008). Consistent with such a view, it has been shown that the WM delay period signal in monkeys lateral pFC was significantly attenuated when the monkey had to covertly attend a spatial position during maintenance (Watanabe & Funahashi, 2014; Lebedev, Messinger, Kralik, & Wise, 2004). Although activity silent mechanisms might have been at play in these studies, it is important to note that WM activity was weak, but still noticeable. Similarly, Kornblith, Quiroga, Koch, Fried, and Mormann (2017) demonstrated that, although most of the visually selective neurons in medial-temporal lobe ceased to encode image information upon presentation of a subsequent image, 8% of neurons continued to carry image-specific information. It is thus possible that WM maintenance in the dual-task condition was subserved by weak neuronal activity, activity insufficient to drive reconstruction of population-level CTFs at the level of the scalp, but sufficient for relatively accurate recall. An alternative possibility is that participants dropped the memory location from WM, performed the intervening task, and then retrieved the memory location from long-term memory at the end of the trial. After all, encoding into long-term memory is a continuous process that is active even during a “WM” task; given a very short delay period and the benefits of recency, it is plausible that participants could have implemented such a strategy. Under conditions of relatively brief interruptions, alpha-based activity patterns may be sufficient to initially implement and then regularly service the memory engram but do not need to be continuously available. Thus, preserved memory performance in the dual-task condition (during which the alpha memory representation was briefly interrupted) does not necessarily entail an explanation based on “activity silent” mechanisms that are distinct from those encoded into long-term memory. Further work is required to distinguish between activity-silent and long-term memory explanations of these findings. That said, our findings do show that items outside the focus of attention are remembered with less precision than those maintained in the focus of attention, consistent with the idea that that the focus of attention, through sustained neuronal firing, enhances the memory representation.

Another important aspect of our data is that the switch in alpha-band topography was initiated in anticipation of the target display. Apparently, observers prioritized the external location over the memory location in advance of the actual display onset. Behavioral estimates suggest that it takes around 300–600 msec to disengage attention from one location and fully reengage it at a new location (Cheal, Lyon, & Gottlob, 1994; Duncan, Ward, & Shapiro, 1994) and cortical shifts of attention appear to follow the same time course (Foster et al., 2017; Müller, Teder-Sälejärvi, & Hillyard, 1998). This supports accounts suggesting that endogenous attention has no high-speed switching mechanism (Theeuwes, Godijn, & Pratt, 2004). In our paradigm, this meant that attention needed to switch to the cued location before target onset to process the target in time before it was masked. The diverging CTFs in the single- and dual-task conditions suggest that observers were aware of this limitation and chose to switch attention in time, even though it meant taking cognitive resources away from the memorized location during the delay period. Importantly, this shows that the diversion of attention was endogenously initiated and not driven by the presentation of the intervening stimuli.

In addition to spatially selective alpha-band activity, which only tracked the prioritized location, we also found that evoked power in the theta-band supported reliable

reconstruction of the task-relevant locations. In contrast to alpha-band activity, after memory display onset these evoked theta CTFs simultaneously carried location-specific information about both the to-be-memorized and the cued location. This effect was especially clear in the dual-task condition, but there was even a small hint in the single-task condition. Recent evidence has linked evoked posterior contralateral theta activity to the N2pc (Dowdall et al., 2012). Our data suggest that the topographic distribution of theta activity not only carries hemifield-specific information but can also track the specific location that is selected. As has been argued by Fahrenfort, Grubert, Olivers, and Eimer (2017), spatial IEMs therefore provide a promising extension to N2pc paradigms, because researchers are no longer limited to the lateralized design.

To conclude, we showed that alpha-based tuning functions shift from reflecting a memorized location to a covertly attended location, when observers are required to perform an attention task during the delay period of a spatial WM task. This moment-by-moment trade-off indicates a common oscillatory mechanism underlying spatial WM and attention.

Acknowledgments

This research was supported by a European Research Council (ERC) advanced grant (ERC-2012-AdG-323413) to J. T., an ERC consolidator grant (ERC-2013-CoG-615423) to C. N. L. O., and NIMH grant 2R01MH087214-06A1 to E. A. D. v. M. contributed to design, collected the data, performed the analyses, and contributed most of the writing. Both C. N. L. O. and E. A. closely supervised the project, were involved in design and writing, and share senior (last) authorship. J. J. F. and D. W. S. aided in the analyses and contributed to writing. J. T. contributed to general design and writing.

References

Awh E, Jonides J. Spatial selective attention and spatial working memory. Attentive Brain. 1998; 12:353–380.

Awh E, Jonides J. Overlapping mechanisms of attention and spatial working memory. Trends in Cognitive Sciences. 2001; 5:119–126. [PubMed: 11239812]

Awh E, Jonides J, Reuter-Lorenz PA. Rehearsal in spatial working memory. Journal of Experimental Psychology: Human Perception and Performance. 1998; 24:780. [PubMed: 9627416]

Awh E, Smith EE, Jonides J. Human rehearsal processes and the frontal lobes: PET evidence. Annals of the New York Academy of Sciences. 1995; 769:97–118. [PubMed: 8595047]

Brouwer GJ, Heeger DJ. Decoding and reconstructing color from responses in human visual cortex. Journal of Neuroscience. 2009; 29:13992–14003. [PubMed: 19890009]

Brouwer GJ, Heeger DJ. Cross-orientation suppression in human visual cortex. Journal of Neurophysiology. 2011; 106:2108–2119. [PubMed: 21775720]

Cheal ML, Lyon DR, Gottlob LR. A framework for understanding the allocation of attention in location-precued discrimination. Quarterly Journal of Experimental Psychology. 1994; 47:699–739.

Cohen, MX. Analyzing neural time series data: Theory and practice. Cambridge, MA: MIT Press; 2014.

de Vries IE, van Driel J, Olivers CN. Posterior alpha EEG dynamics dissociate current from future goals in working memory guided visual search. Journal of Neuroscience. 2017; 37:1591–1603. [PubMed: 28069918]

Dowdall JR, Luczak A, Tata MS. Temporal variability of the N2pc during efficient and inefficient visual search. Neuropsychologia. 2012; 50:2442–2453. [PubMed: 22743179]

Duncan J, Ward R, Shapiro K. Direct measurement of attentional dwell time in human vision. Nature. 1994; 369:313–315. [PubMed: 8183369]

Fahrenfort JJ, Grubert A, Olivers CN, Eimer M. Multivariate EEG analyses support high-resolution tracking of feature-based attentional selection. Scientific Reports. 2017; 7:1886. [PubMed: 28507285]

Foster JJ, Bsales EM, Jaffe RJ, Awh E. Alpha-band activity reveals spontaneous representations of spatial position in visual working memory. Current Biology. 2017; doi: 10.1016/j.cub.2017.09.031

Foster JJ, Sutterer DW, Serences JT, Vogel EK, Awh E. The topography of alpha-band activity tracks the content of spatial working memory. Journal of Neurophysiology. 2016; 115:168–177. [PubMed: 26467522]

Foster JJ, Sutterer DW, Serences JT, Vogel EK, Awh E. Alpha-band oscillations enable spatially and temporally resolved tracking of covert spatial attention. Psychological Science. 2017; 28:929–941. [PubMed: 28537480]

Gould IC, Rushworth MF, Nobre AC. Indexing the graded allocation of visuospatial attention using anticipatory alpha oscillations. Journal of Neurophysiology. 2011; 105:1318–1326. [PubMed: 21228304]

Gramfort A, Luessi M, Larson E, Engemann DA, Strohmeier D, Brodbeck C, et al. MEG and EEG data analysis with MNE-Python. Frontiers in Neuroscience. 2013; 7:267. [PubMed: 24431986]

Hollingworth A, Maxcey-Richard AM. Selective maintenance in visual working memory does not require sustained visual attention. Journal of Experimental Psychology: Human Perception and Performance. 2013; 39:1047. [PubMed: 23067118]

Kaernbach C. Simple adaptive testing with the weighted up-down method. Attention, Perception, & Psychophysics. 1991; 49:227–229.

Kelly SP, Lalor EC, Reilly RB, Foxe JJ. Increases in alpha oscillatory power reflect an active retinotopic mechanism for distracter suppression during sustained visuospatial attention. Journal of Neurophysiology. 2006; 95:3844–3851. [PubMed: 16571739]

Kiyonaga A, Egner T. Working memory as internal attention: Toward an integrative account of internal and external selection processes. Psychonomic Bulletin & Review. 2013; 20:228–242. [PubMed: 23233157]

Kornblith S, Quiroga RQ, Koch C, Fried I, Mormann F. Persistent single-neuron activity during working memory in the human medial temporal lobe. Current Biology. 2017; 27:1026–1032. [PubMed: 28318972]

LaRocque JJ, Lewis-Peacock JA, Drysdale AT, Oberauer K, Postle BR. Decoding attended information in short-term memory: An EEG study. Journal of Cognitive Neuroscience. 2013; 25:127–142. [PubMed: 23198894]

LaRocque JJ, Riggall AC, Emrich SM, Postle BR. Within-category decoding of information in different attentional states in short-term memory. Cerebral Cortex. 2016; 27 bhw283.

Lebedev MA, Messinger A, Kralik JD, Wise SP. Representation of attended versus remembered locations in prefrontal cortex. PLoS Biology. 2004; 2:e365. [PubMed: 15510225]

Lewis-Peacock JA, Drysdale AT, Oberauer K, Postle BR. Neural evidence for a distinction between short-term memory and the focus of attention. Journal of Cognitive Neuroscience. 2012; 24:61–79. [PubMed: 21955164]

Lins OG, Picton TW, Berg P, Scherg M. Ocular artifacts in EEG and event-related potentials I: Scalp topography. Brain Topography. 1993; 6:51–63. [PubMed: 8260327]

Luck SJ, Hillyard SA. Electrophysiological evidence for parallel and serial processing during visual search. Perception & Psychophysics. 1990; 48:603–617. [PubMed: 2270192]

Maris E, Oostenveld R. Nonparametric statistical testing of EEG- and MEG-data. Journal of Neuroscience Methods. 2007; 164:177–190. [PubMed: 17517438]

Mathôt S, Schreij D, Theeuwes J. OpenSesame: An open-source, graphical experiment builder for the social sciences. Behavior Research Methods. 2012; 44:314–324. [PubMed: 22083660]

Medendorp WP, Kramer GF, Jensen O, Oostenveld R, Schoffelen J-M, Fries P. Oscillatory activity in human parietal and occipital cortex shows hemispheric lateralization and memory effects in a delayed double-step saccade task. Cerebral Cortex. 2007; 17:2364–2374. [PubMed: 17190968]

Mongillo G, Barak O, Tsodyks M. Synaptic theory of working memory. Science. 2008; 319:1543–1546. [PubMed: 18339943]

Müller MM, Teder-Sälejärvi W, Hillyard SA. The time course of cortical facilitation during cued shifts of spatial attention. Nature Neuroscience. 1998; 1:631–634. [PubMed: 10196572]

Olivers CN. Interactions between visual working memory and visual attention. Frontiers in Bioscience. 2008; 13:1182–1191. [PubMed: 17981622]

Olivers CN, Peters J, Houtkamp R, Roelfsema PR. Different states in visual working memory: When it guides attention and when it does not. Trends in Cognitive Sciences. 2011; 15:327–334. [PubMed: 21665518]

Postle BR. Working memory as an emergent property of the mind and brain. Neuroscience. 2006; 139:23–38. [PubMed: 16324795]

Rihs TA, Michel CM, Thut G. Mechanisms of selective inhibition in visual spatial attention are indexed by α-band EEG synchronization. European Journal of Neuroscience. 2007; 25:603–610. [PubMed: 17284203]

Rose NS, LaRocque JJ, Riggall AC, Gosseries O, Starrett MJ, Meyering EE, et al. Reactivation of latent working memories with transcranial magnetic stimulation. Science. 2016; 354:1136–1139. [PubMed: 27934762]

Samaha J, Sprague TC, Postle BR. Decoding and reconstructing the focus of spatial attention from the topography of alpha-band oscillations. Journal of Cognitive Neuroscience. 2016; 28:1090–1097. [PubMed: 27003790]

Stokes MG. 'Activity-silent' working memory in prefrontal cortex: A dynamic coding framework. Trends in Cognitive Sciences. 2015; 19:394–405. [PubMed: 26051384]

Suchow JW, Brady TF, Fougnie D, Alvarez GA. Modeling visual working memory with the MemToolbox. Journal of Vision. 2013; 13:9.

Theeuwes J, Godijn R, Pratt J. A new estimation of the duration of attentional dwell time. Psychonomic Bulletin & Review. 2004; 11:60–64. [PubMed: 15116987]

Theeuwes J, Olivers CN, Chizk CL. Remembering a location makes the eyes curve away. Psychological Science. 2005; 16:196–199. [PubMed: 15733199]

van Dijk H, van der Werf J, Mazaheri A, Medendorp WP, Jensen O. Modulations in oscillatory activity with amplitude asymmetry can produce cognitively relevant event-related responses. Proceedings of the National Academy of Sciences. 2010; 107:900–905.

Watanabe K, Funahashi S. Neural mechanisms of dual-task interference and cognitive capacity limitation in the prefrontal cortex. Nature Neuroscience. 2014; 17:601–611. [PubMed: 24584049]

Woodman GF, Vogel EK, Luck SJ. Visual search remains efficient when visual working memory is full. Psychological Science. 2001; 12:219–224. [PubMed: 11437304]

Zhang W, Luck SJ. Discrete fixed-resolution representations in visual working memory. Nature. 2008; 453:233–235. [PubMed: 18385672]

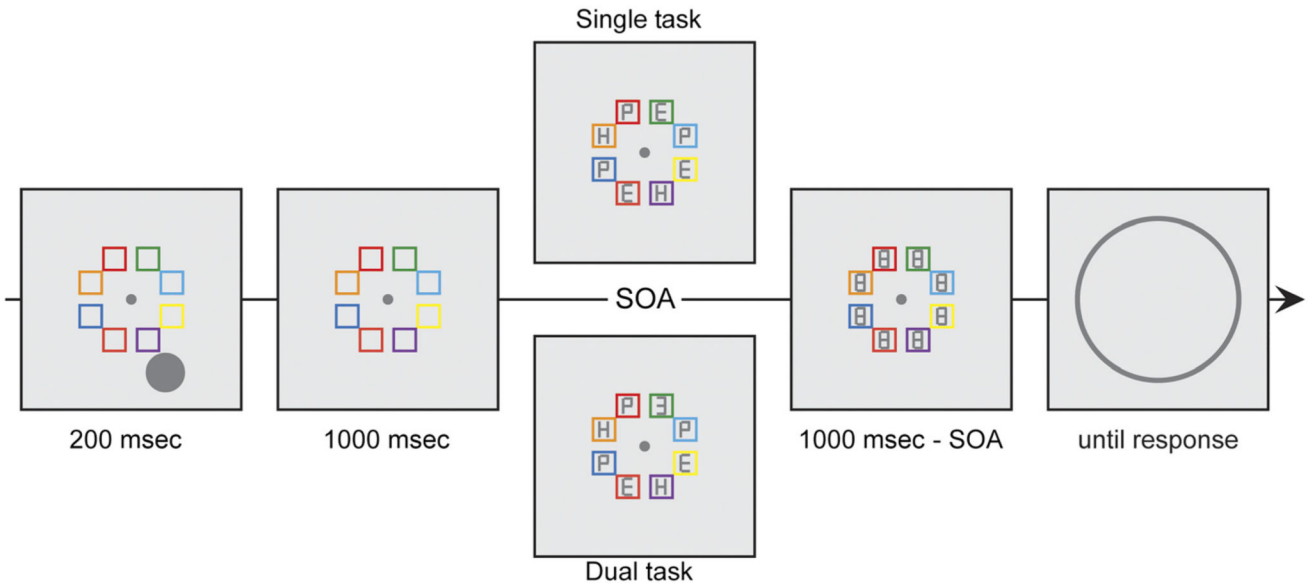

Figure 1.

Spatial WM task: In both conditions, participants had to remember the location of gray circle while maintaining fixation. After a delay, observers reported the angular location of this circle by clicking on the perimeter of a rim. Before giving the response, in the dual-task condition, observers performed a spatial attention task in which they indicated the digit (2, 3, or 5) that was presented in one of the colored boxes. Participants were told which colored box would contain a digit; the color remained fixed throughout the experiment and had a validity of 87.5%. Participants had 1000 msec to respond, but the displays were masked after a predefined SOA, which was determined offline for each participant. Displays in the single-task conditions were identical, but observers were instructed to ignore the displays associated with the intermediate task. Single- and dual-task conditions were blocked.

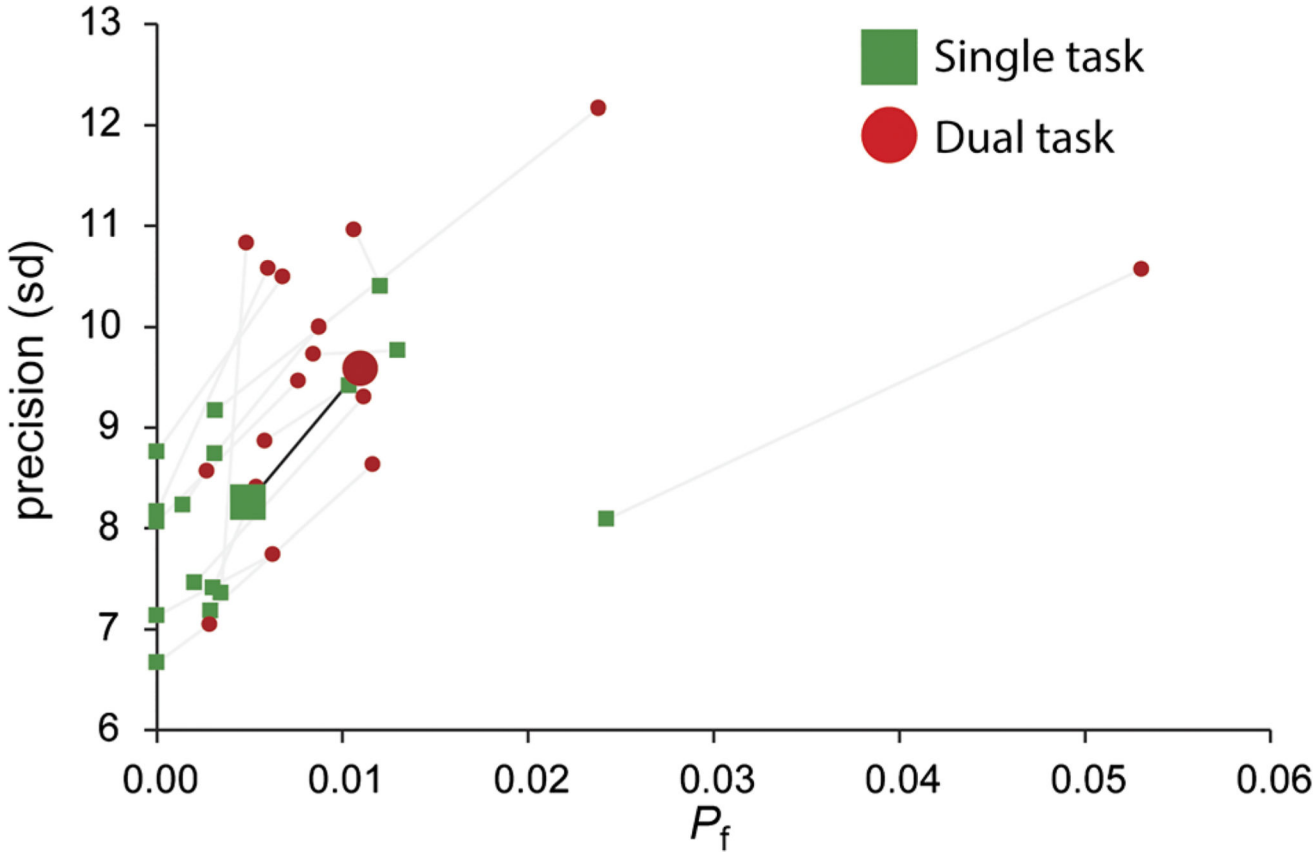

Figure 2.

Mnemonic precision (sd) and the probability of forgetting the remembered location (P_f) as a function of condition. Although there was a cost of covert shifts of attention, indicated by significant effects on both parameters, recall performance in the dual-task condition was nevertheless quite accurate.

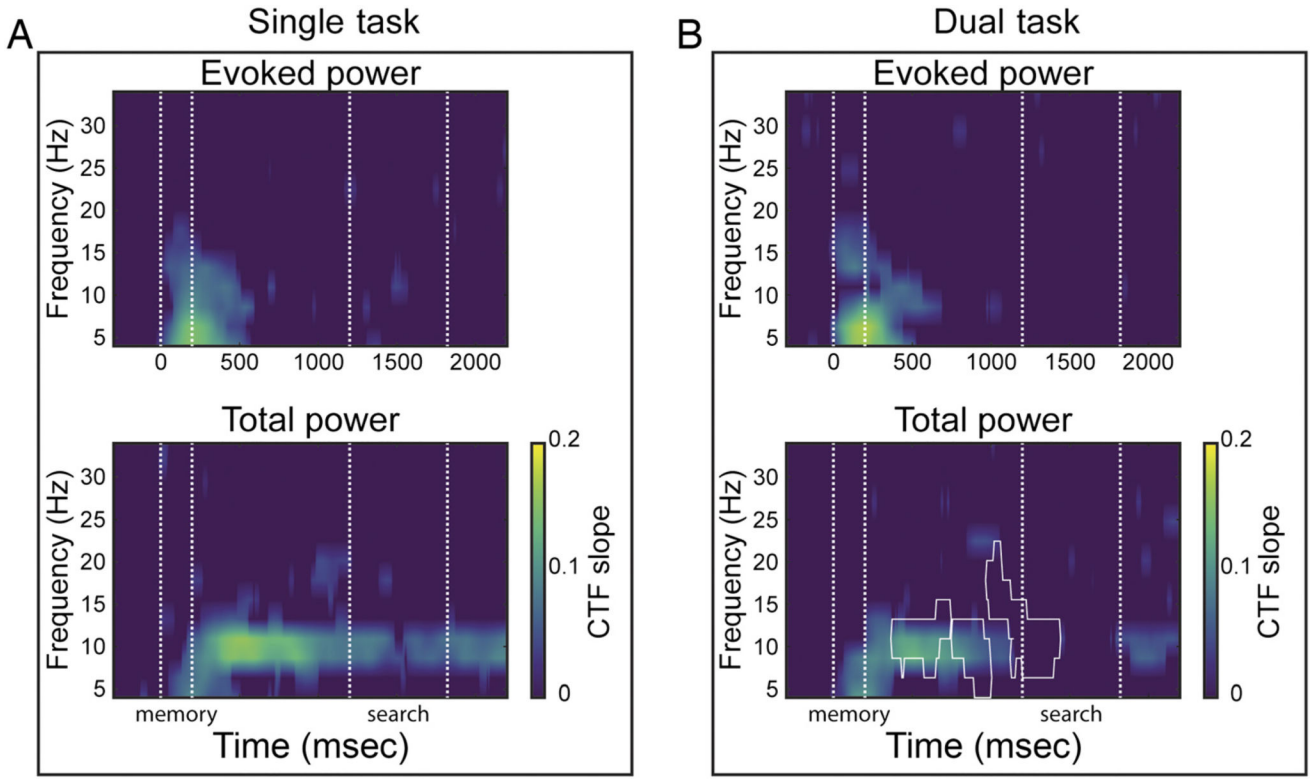

Figure 3.

Identification of the remembered location via evoked (top) and total (bottom) power across frequency bands as indexed by CTF slopes. The CTF slope is a measure of CTF selectivity that quantifies the location-specific activity in the topographic distribution of power. Individual figures show CTFs slopes for single-task (A) and dual-task conditions (B). Points at which CTF slope was not reliably above zero as determined by a permutation test are set to zero (purple). White outline denotes significant slope difference between single- and dual-task conditions ($p < .05$). Across figures, $t = 0$, $t = 200$, $t = 1200$ represent the memory display onset, start of the delay period, and target display onset, respectively. Areas marked by the white dotted lines mark the memory display (onset till offset) and the attention task (target display onset until average RT).

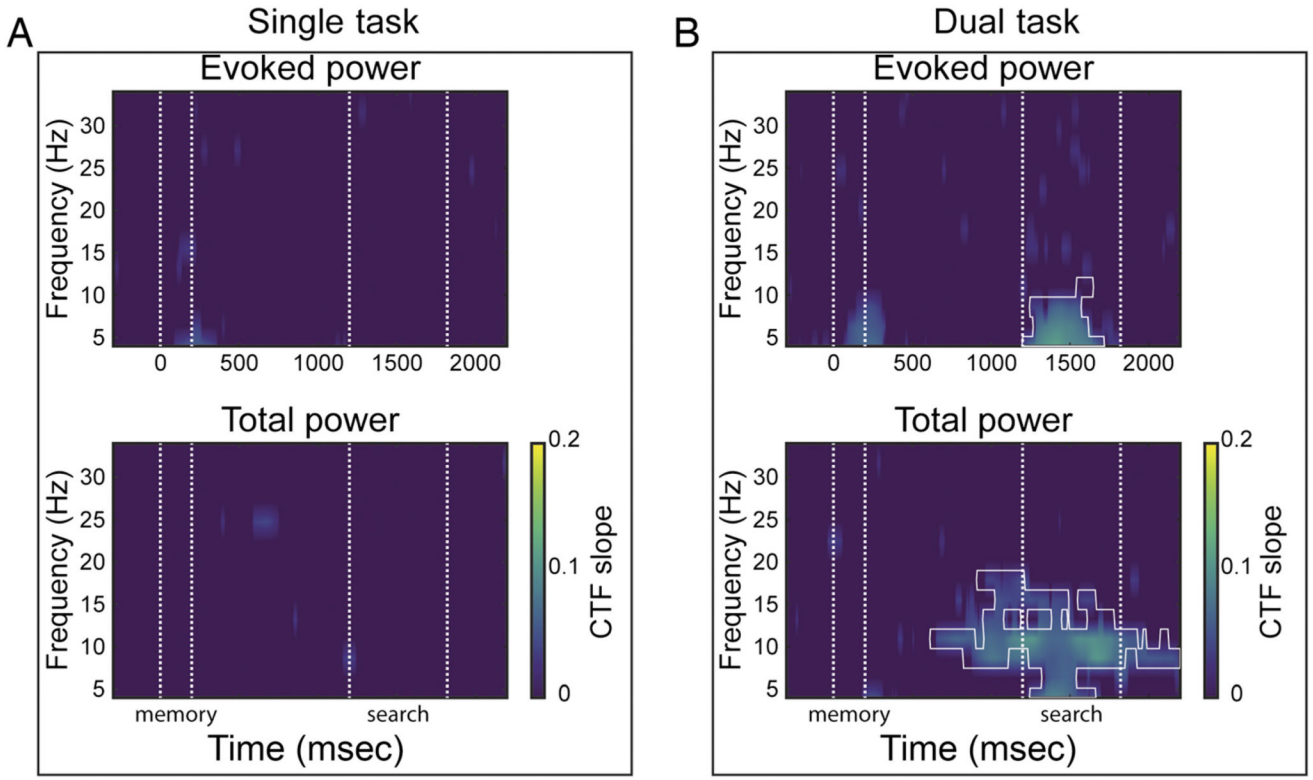

Figure 4.

Identification of the cue location via evoked (top) and total (bottom) power across frequency bands as indexed by CTF slopes. Individual figures show CTFs slopes for single-task (A) and dual-task conditions (B). Points at which CTF slope was not reliably above zero as determined by a permutation test are set to zero (purple). White outline denotes significant slope difference between single- and dual-task conditions ($p < .05$).

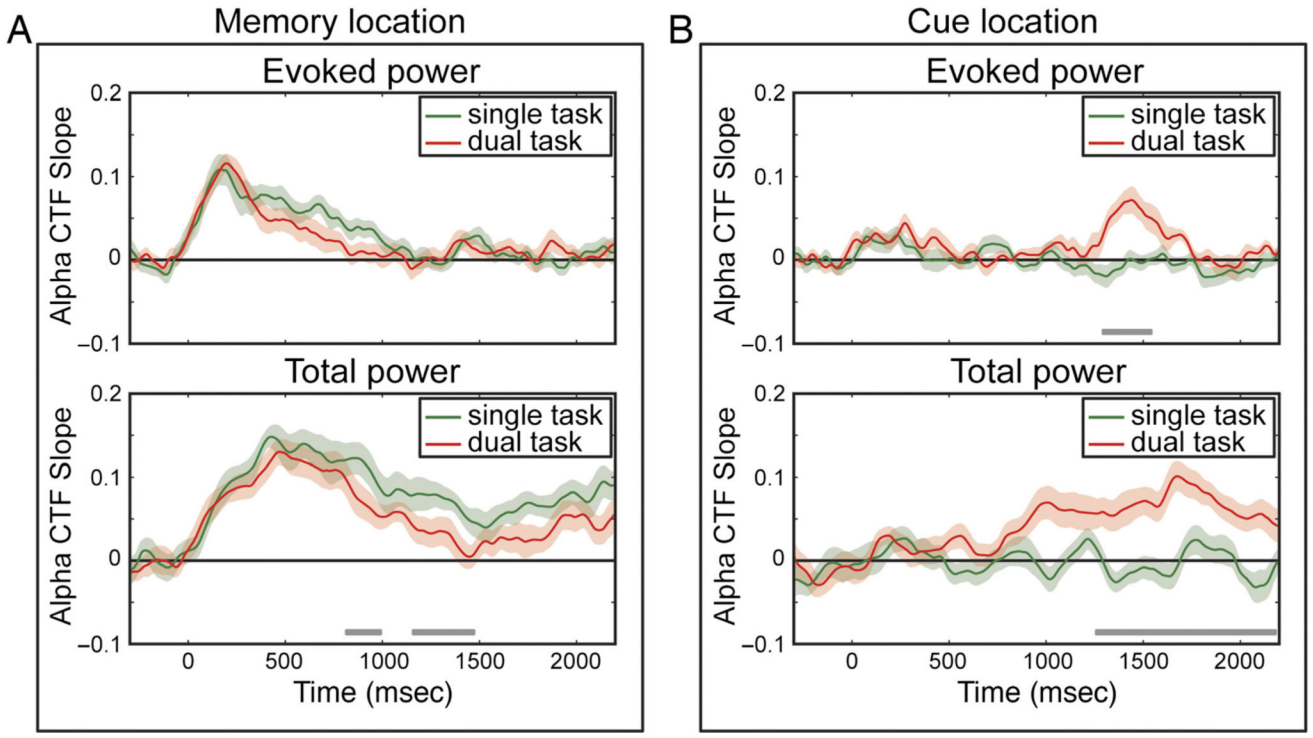

Figure 5.

Alpha evoked power and total power CTF selectivity across conditions and attended locations. Individual figures show CTF slopes for both conditions for the memory location (A) and the cue location (B). Shaded error bars reflect bootstrapped *SEM*. Time points where CTF slope significantly differed, as indicated with a cluster-based permutation test ($p < .05$) are indicated with gray bars.

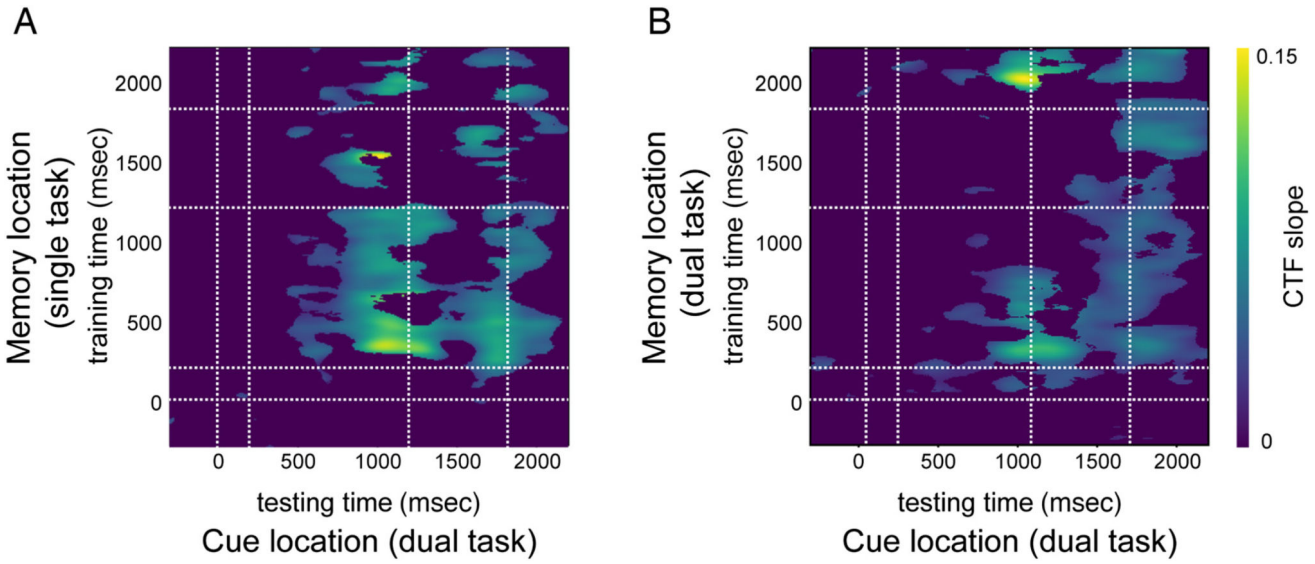

Figure 6.

Generalization across time CTF slopes after cross-training between memory locations and cue locations in the dual-task blocks, using memory locations from the single task block (A) and memory locations from the dual-task blocks (B). Points at which CTF slope was not reliably above zero as determined by a permutation test ($p < .01$) are set to zero (purple). Areas marked by the white dotted lines mark the memory display (onset till offset) and the attention task (target display onset until average RT).